Int. J. Dev. Biol. 41: 655-666 (1997)

Original Article

Homeobox genes from clusters A and B demonstrate characteristics of temporal colinearity and differential restrictions in spatial expression domains in the branching mouse lung

RICHARD MOLLARD* and MARIE DZIADEK[1]

Institute of Reproduction and Development, Monash University, Clayton, Victoria, Australia

ABSTRACT Lung branching morphogenesis is accomplished by reciprocal morphogenetic interactions between the epithelium and its mesenchyme. In order to better understand the molecular mechanisms regulating these interactions in time and space, the expression patterns of *Hox* genes isolated exclusively from the branching region of the developing lung have been investigated. Reverse transcriptase PCR identified *Hoxa-1, Hoxa-3, Hoxa-5, Hoxb-3, Hoxb-4, Hoxb-6, Hoxb-7,* and *Hoxb-8* transcripts from within this tissue at 11.5 day post coitum (E11.5). Northern blot, *in situ* hybridization and PCR analyses demonstrated qualitative and quantitative differences in expression patterns for each gene assessed in this region thus providing evidence for *Hox* gene temporal colinearity. Furthermore, although not within the context of strict anteroposterior definition, *Hox* genes located within a more 5' region in both clusters were found to have greater spatial expression constrictions when compared to their more 3' counterparts. These *Hox* genes were also differentially expressed both between and within specific germ cell lineage derivatives. Such patterns of expression suggest that *Hox* genes play a role in the specification and maturation of lung cell lineage derivatives throughout the pseudoglandular, canalicular and terminal sac phases of lung development.

KEY WORDS: *Hox genes, embryonic lung development, branching morphogenesis, distalbud, interbud, colinearity*

Introduction

The mechanisms governing branching morphogenesis during embryogenesis have been studied extensively at the cellular level in a variety of systems including the developing lung, kidney, salivary gland, and mammary gland (Saxén *et al.*, 1976; Bernfield, 1981; Lawson, 1983; Hilfer *et al.*, 1985). Such studies have revealed the indispensability of epithelial/mesenchymal interactions for correct branching morphogenesis and have demonstrated the existence of a functional heterogeneity within the branching mesenchyme which guides both epithelial bud outgrowth and cleft formation/stabilization.

The actions of both soluble and insoluble transmissible signals have been shown to represent important effectors of epithelial/mesenchymal interactions (Ekblom *et al.*, 1994; Nogowa and Ito, 1995). Extracellular morphoregulatory molecules of this type are arranged within spatially restricted compartments of the branching lung and include growth factors and components of the extracellular matrix (ECM). Indeed, recent studies involving the addition of specific antibodies and antisense oligodeoxynucleotides to culture systems and the production of transgenic animals have directly demonstrated their functional significance both *in vitro* and *in vivo* (Seth *et al.*, 1993; Peters *et al.*, 1994; Kadoya *et al.*, 1995; Schuger *et al.*, 1995; Souza *et al.*, 1995; Bellusci *et al.*, 1996).

The definition of these modulators of cellular behavior have increased considerably a mechanistic understanding of pattern formation during lung organogenesis. The conceptualization of such patterning, however, is only made possible by the elucidation of factors specifying positional information within a framework of cell population subsets and specific lineage derivatives (James and Kazenwadel, 1991). In this context, it is of interest that retinoic acid (RA) possesses the ability to change the positional information endowed upon a number of developing and regenerating systems and that compound null-

Abbreviations used in this paper: ECM, extracellular matrix; RA, retinoic acid; RT-PCR, reverse transcriptase-polymerase chain reaction; E11.5, embryonic day 11.5; PSL, photosensitive light units; ANT-C, Antennapedia complex; Ubx, Ultrabithorax; abd-A, abdominal-A.

***Address for reprints:** Institut de Génétique et de Biologie Moléculaire et Cellulaire, CNRS/INSERM/ULP, Collège de France, BP 163, F-67404 Illkirch-Cedex, C.U. de Strasbourg, France. FAX: 33.388653203. e-mail: mollard @ titus. u-strasbg.fr

[1]**Present address:** Department of Anatomy and Cell Biology, University of Melbourne, Parkville, Victoria 3052, Australia.

0214-6282/97/$05.00

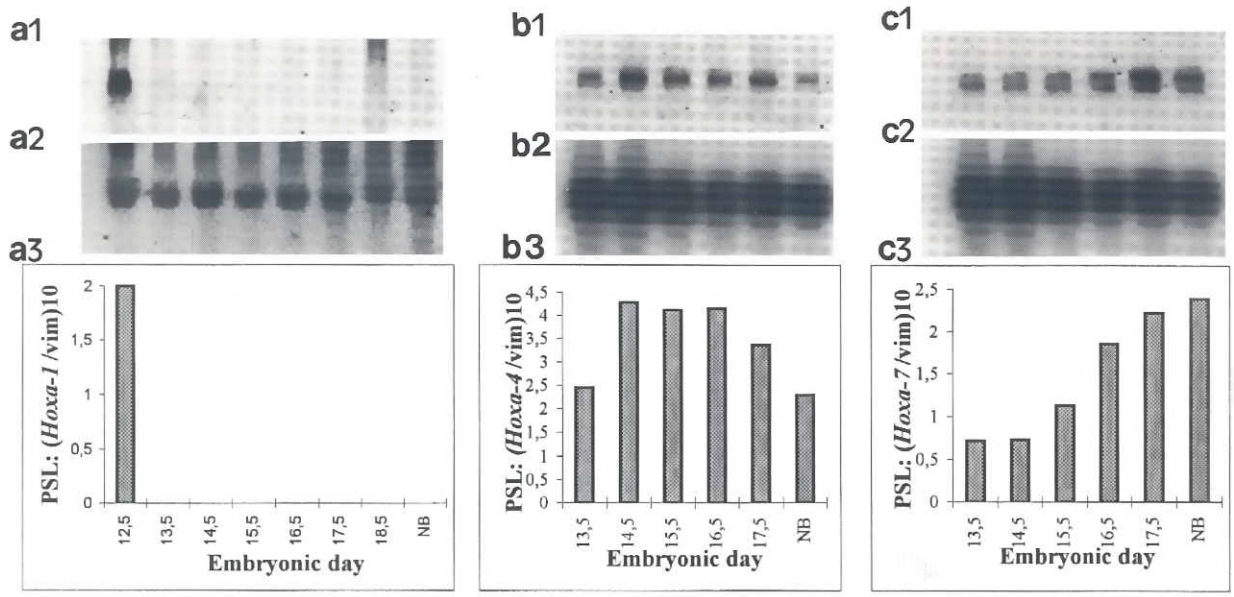

Fig. 1. Temporal expression patterns of *HoxA* genes during lung development as determined by Northern blot analyses. (a1, b1 and c1) *Phosphoimaging of the 2.2-2.4 kb Hoxa-1 (30 μg of total lung RNA/track), 1.7 kb Hoxa-4 and 2.1-2.4 kb Hoxa-7 (2 μg of lung mRNA/track) transcripts, respectively.* **(a2, b2 and c2)** *The respective membranes reprobed for the 1.8 kb vimentin transcripts.* **(a3)** *The relative amounts of (Hoxa-1/vimentin)x10.* **(b3)** *The relative amount of (Hoxa-4/vimentin)x10. Quadratic regression analysis demonstrates a significant increase and then decrease of slope with time (P<0.05).* **(c3)** *The relative amount of (Hoxa-7/vimentin)x10. Linear regression analysis demonstrates a significant slope increase with time (P<0.001). NB, newborn.*

mutants of the retinoic acid receptors α and β2 display agenesis/severe hypoplasia of the lung (Mendelsohn *et al.*, 1994). Whether RA controls branching morphogenesis by affecting the expression of proposed lung morphoregulatory genes such as laminin β1 or integrin β1 (Vasios *et al.*, 1989; Roman *et al.*, 1991; Ross *et al.*, 1994; Schuger *et al.*, 1995) is unknown, however, it does regulate expression of *Homeobox (Hox)* genes, members of a transcriptional regulatory family specifying positional information and pattern formation during embryogenesis and implicated in the epithelial/mesenchymal interactions that mediate growth (Izpisúa-Belmonte *et al.*, 1992; Dollé *et al.*, 1993; Yokouchi *et al.*, 1995).

Identified by virtue of their homology to *Drosophila* homeotic sequences, the vertebrate *Hox* gene family has been shown to comprise 39 members. The specific timing and spatial organization of each gene's expression domain is thought to translate genetic information into a combinatorial code, instructive to the definition of individually confined areas along the axes of developing systems. Such an effect may be accomplished by delineating distinct subsets of cells necessary for the compartmentalized regulation of target genes such as cell adhesion molecules, growth factors and/or components of the extracellular matrix (Jones *et al.*, 1992; Capovilla *et al.*, 1994; Duboule, 1995).

Homeotic genes have been proposed to determine *Drosophila* salivary gland anlage formation by controlling the downstream genes involved in its morphogenesis (Panzer *et al.*, 1992). The demonstration that morphogenetic processes such as the formation of the second midgut restriction of *Drosophila* is attributable to an intricate relationship between homeotic genes and the transforming growth factor β homolog decapentaplegic (Capovilla *et al.*, 1994), further demonstrates the role of *Hox* genes in the specification of cellular identity during organogenesis. Together with the evidence that expression of both *Hoxa-1* and *Hoxc-6* alters concomitant to changes in the proliferative status of ectodermal cells within preneoplastic and neoplastic mouse mammary glands (Friedmann *et al.*, 1994), these studies suggest that certain *Hox* genes may control the molecular processes leading to morphogenesis of embryonic glandular organs.

The expression of a number of *Hox* genes has previously been reported during different stages of lung development (Krumlauf *et al.*, 1987; Graham *et al.*, 1988; Gaunt *et al.*, 1989; Bernacki *et al.*, 1992; Sham *et al.*, 1992; Behringer *et al.*, 1993; Cardoso, 1995;

TABLE 1

THE IDENTITY AND FREQUENCY OF *Hox* GENE FAMILY MEMBERS SUBCLONED FROM THE BRANCHING REGION OF THE E11.5 MOUSE LUNG AFTER RT-PCR

Homeobox sequence	Frequency of cloning	Reference
Hoxa-1	28	Baron *et al.*, 1987
Hoxa-3	34	Lonai *et al.*, 1987
Hoxa-5	25	Odenwald *et al.*, 1987
Hoxb-3	28	Sham *et al.*, 1992
Hoxb-4	47	Graham *et al.*, 1988
Hoxb-6	56	Shen *et al.*, 1991
Hoxb-7	9	Meijlink *et al.*, 1987
Hoxb-8	6	Kongsuwan *et al.*, 1988

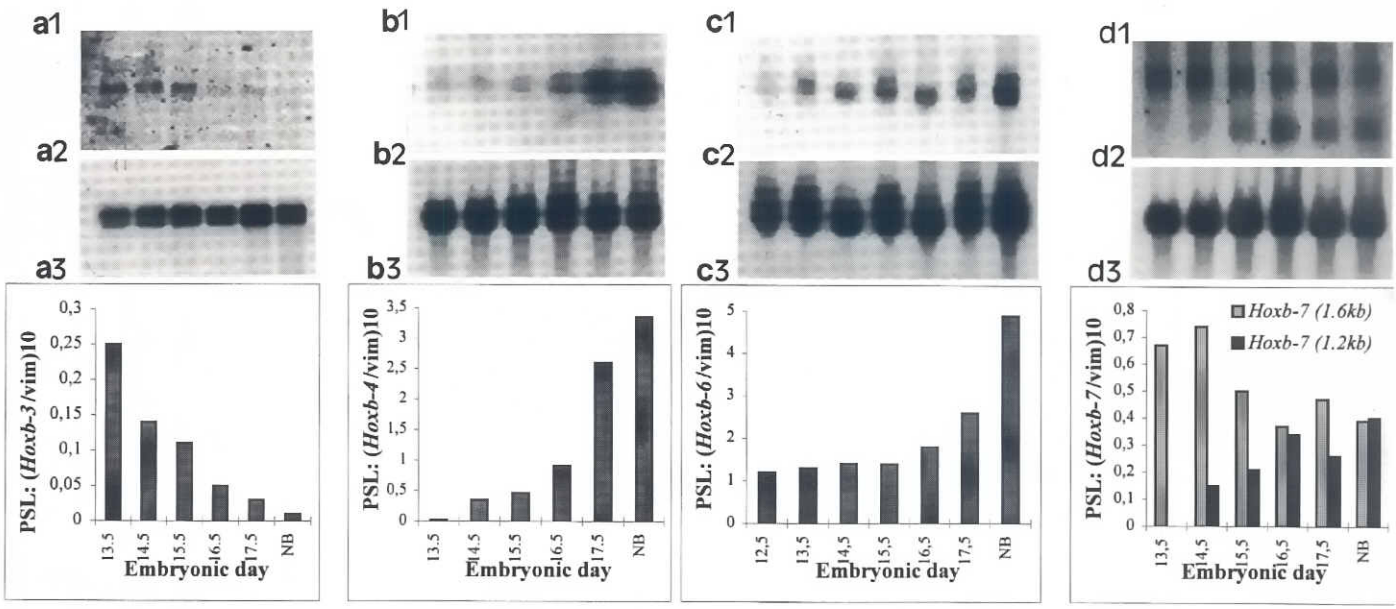

Fig. 2. Temporal expression patterns of *HoxB* genes during lung development. (a1, b1, c1 and d1) *Phospho-imaging of the 6.8 kb Hoxb-3 (30 μg of total lung RNA/track), 2.1 kb Hoxb-4 (2 μg of lung mRNA/track), 1.2-1.4 kb Hoxb-6 (30 μg of total lung RNA/track) and 1.2-1.4 kb and 1.6 kb Hoxb-7 (2 μg of lung mRNA/track) transcripts, respectively.* **(a2, b2, c2 and d2)** *The respective membranes reprobed for vimentin.* **(a3)** *The relative amounts of (Hoxb-3/vimentin)x10. Linear regression analysis demonstrates a significant decrease in slope with time (P<0.005).* **(b3 and c3)** *The relative amounts of (Hoxb-4/vimentin)x10 and (Hoxb-6/vimentin)x10, respectively. Linear regression analyses demonstrate a significant increase in slopes with time (P<0.01 and P<0.001, respectively).* **(d3)** *The relative amounts of (Hoxb-7/vimentin)x10. Linear regression analyses demonstrate a significant decrease in the slope of the 1.6 kb transcript (P< 0.05) and a significant increase in the slope of the smaller transcript (P<0.01) with time. NB, newborn.*

Bogue *et al.*, 1996). Furthermore, the expression of a number of *Hox* genes within lung tissue has been reported as sensitive to the application of RA *in vitro* (Bernacki *et al.*, 1992; Bogue *et al.*, 1994; Cardoso *et al.*, 1995). A series of experiments involving a reverse transcriptase-polymerase chain reaction (RT-PCR) based strategy (James and Kazenwadel, 1991) and Northern, *in situ* hybridization and quantitative PCR analyses was, therefore, designed to identify and characterize the expression patterns of homeobox gene family members during early lung development. These investigations concentrated exclusively on lung regions involved in branching morphogenesis and not those involved in the maturation of more proximal lung structures, such as the trachea, due to the presumption that the development of these two regions is regulated by distinct morphogenetic mechanisms.

Results

The identification of Hox genes within the E11.5 bronchiolar lung

The RT-PCR strategy, when applied to mRNA isolated from the branching region of E11.5 mouse lungs, enabled the identification of 8 individual *Hox* sequences: *Hoxa-1*, *Hoxa-3*, *Hoxa-5*, *Hoxb-3*, *Hoxb-4*, *Hoxb-6*, *Hoxb-7* and *Hoxb-8* (Table 1). All *Hox* genes identified by this study are ANT-C/ *Ubx/abd-A* - type *Hox* genes of the *HoxA* and *HoxB* clusters. Although each gene demonstrated a different frequency of cloning, such values cannot be presumed representative of relative expression levels (He *et al.*, 1989).

Hox gene temporal expression patterns in the bronchiolar lung

Linear regression analyses after repetitive Northern blot and phospho-imaging analyses of 28S and vimentin mRNA demonstrated no significant difference in their ratio from E12.5 to birth in lung tissue dissected free from presumptive trachea (data not shown). Northern blot analyses were then performed in order to determine temporal dynamics in the expression levels of individual *Hox* genes, relative to the expression of vimentin, within the branching lung. Tissue was taken from E12.5 or 13.5 day due to the technical difficulty involved in obtaining sufficient amounts for Northern analysis from earlier time points. A single 2.2-2.4 kb *Hoxa-1* transcript was detected in RNA obtained from E12.5 lung buds. No transcripts were detected at later time points (Fig. 1a). A single 1.7 kb *Hoxa-4* transcript was detected from E13.5 to birth. A significant increase in expression of this transcript was observed between E13.5 and E14.5. Expression appeared to plateau from E14.5 until E16.5. A significant decrease was then observed between approximately E16.5 and birth ($P<0.05$) (Fig. 1b). A single 2.1-2.4 kb *Hoxa-7* transcript was detected from E13.5 to birth. Expression showed a significant and progressive 3 fold increase throughout this period ($P<0.001$) (Fig. 1c).

A single 6.8 kb *Hoxb-3* transcript was detected at E13.5. A significant and progressive decrease in the amount of this transcript was observed concomitant to development, disappearing in the new born sample ($P<0.005$) (Fig. 2a). A single 2.1 kb *Hoxb-4* transcript was detected from E13.5 to birth; a significant increase

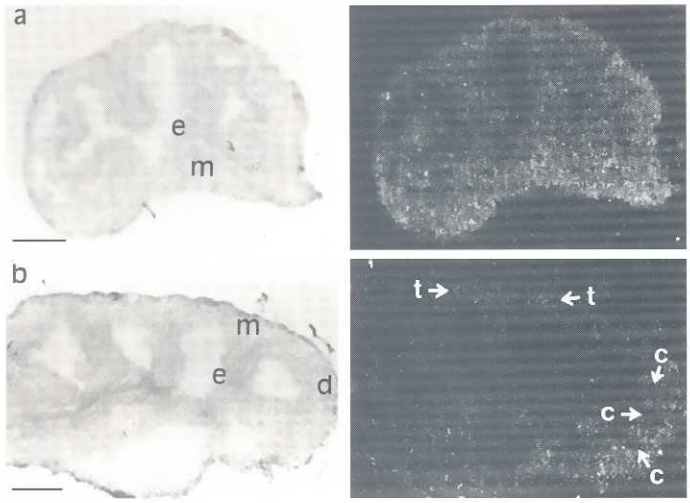

Fig. 3. *In situ* hybridization analyses of *HoxA* spatial expression in the E11.5 mouse lung. *(e) epithelium, (m) mesenchyme.* **(a)** *Light and dark field illuminations of a Hoxa-1 antisense probe. Hybridization can be seen within the epithelial and mesenchymal layers. Hybridization appears higher in the mesenchyme than in the epithelium.* **(b)** *Light and dark field illuminations of a Hoxa-4 antisense probe. Hybridization can be seen within the mesenchyme. Epithelial cells show little or no hybridization. Greatest hybridization is seen in the distal mesenchyme corresponding to the most posterior aspect of the lung within the body's anteroposterior axis (d). Within this region, circular groups of cells show weak expression (c). Hybridization is also relatively higher in the mesenchyme associated with the more distal tips (t). Bar, 150 μm.*

in its expression was observed throughout embryological development, especially in the latter stages and into the newborn ($P<0.01$) (Fig. 2b). A single 1.2-1.4 kb *Hoxb-6* transcript was detected from E12.5 until birth. Expression significantly increased during this time ($P<0.001$). This progressive increase in expression was more pronounced during the latter stages of embryological development and later to that of *Hoxb-4* (Fig. 2c). Two *Hoxb-7* transcripts were detected. The transcript of approximately 1.6 kb showed a significant and progressive decrease in expression levels from E13.5 to birth ($P<0.05$). The transcript of approximately 1.2-1.4 kb, which was not present at the earliest time points, subsequently showed a significant and progressive 4 fold increase from E14.5 to birth ($P<0.01$) (Fig. 2d). All detected transcript sizes corresponded to those previously described: *Hoxa-1* (Baron *et al.*, 1987), *Hoxa-4* (Galliot *et al.*, 1989), *Hoxa-7* (Parikh *et al.*, 1995), *Hoxb-3* (Graham *et al.*, 1989), *Hoxb-4* (Shen *et al.*, 1989), *Hoxb-6* (Graham *et al.*, 1989) and *Hoxb-7* (Meijlink *et al.*, 1987; Kongsuwan *et al.*, 1988).

Hox gene spatial expression patterns

In situ hybridization using *Hox* riboprobes was performed to determine specific spatial expression patterns in the branching region of the E11.5 lung. Although expression of *Hoxb-6* has been previously demonstrated by *in situ* hybridization (Gaunt *et al.*, 1989), expression of neither *Hoxa-7*, *Hoxb-4* nor *Hoxb-6* was detectable by *in situ* hybridization in the E11.5 mouse lung bud in our hands (data not shown). *Hoxa-1* expression was found throughout both the epithelial and mesenchymal components of the lung. Higher expression was evident in the mesenchyme as compared to the epithelium (Fig. 3a). *Hoxa-4* expression was detectable in the mesenchyme where higher levels were observed in the more distal regions, especially around the budding tips (Fig. 3b). Small groups of cells which appeared to contain no expression were also observed within the mesenchyme. Weak *Hoxa-4* expression was observed in the epithelium. *Hoxb-3* expression appeared to be uniform throughout the mesenchyme. Weak expression was found in the epithelium (Fig. 4a). *Hoxb-5* expression was highest within the pericapsular mesenchyme and the mesenchyme abutting the epithelial interface. Between these two regions, within the clefts, *Hoxb-5* expression was markedly reduced. Weak *Hoxb-5* expression was observed within the epithelium (Fig. 4b). Very low *Hoxb-7* expression levels were detected in the more distal portions of three sections from only one lung. Whether this expression was specific to the mesenchyme could not be determined (Fig. 4c).

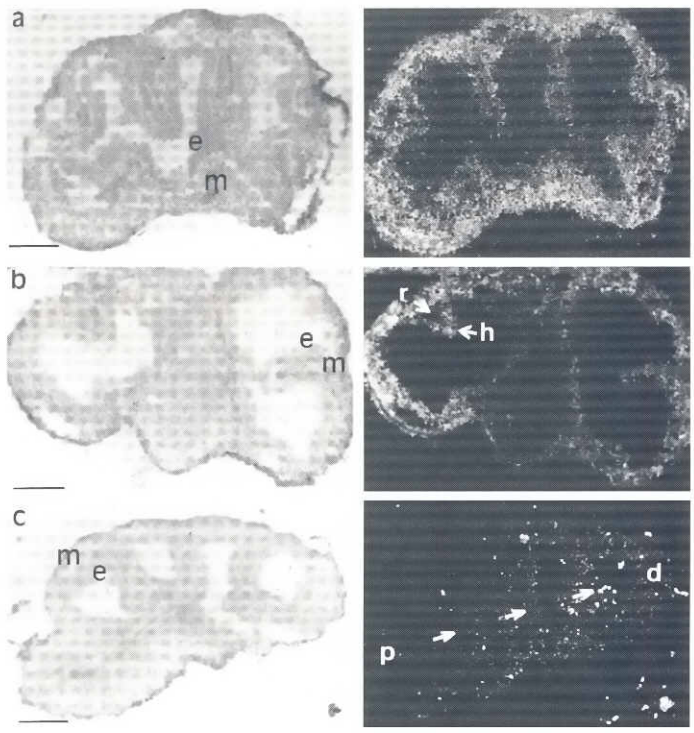

Fig. 4. *In situ* hybridization analyses of *HoxB* spatial expression in the E11.5 mouse lung. *(e) epithelium, (m) mesenchyme.* **(a)** *Light and dark field illuminations of a Hoxb-3 antisense probe. Hybridization can be seen within the mesenchymal layer. Little or no hybridization can be seen within the epithelium.* **(b)** *Light and dark field illuminations of a Hoxb-5 antisense probe. Hybridization can be seen within the mesenchymal layer. Highest hybridization appears to be associated with the mesenchyme of the epithelial interface (h). Hybridization is reduced in the mesenchyme subjacent to the interfacial mesenchyme (r). Weak hybridization appears to be associated with the epithelium.* **(c)** *Light and dark field illuminations of a Hoxb-7 antisense probe. Low levels of hybridization can be seen within the mesenchyme. Hybridization appears to intensify along the proximodistal axis (p->->->-d). Bar, 150 μm.*

Quantitative PCR

Quantitative PCR was used to further analyze *Hox* gene expression within the E11.5 developing lung. Specific levels of expression between the newly formed distalbud regions and the newly formed interbud regions were compared. Distalbud (DB) regions were defined as those which lay distal to the widest margin across the terminal bud. Interbud (IB) regions were defined as those which lay proximal to this margin (see Materials and Methods).

Northern blot analyses demonstrated that vimentin is expressed at relatively equivalent levels in both interbud and distalbud tissues (data not shown). Vimentin PCR primers amplified the expected 550bp band from E11.5 mouse carcass cDNA (Fig. 5). Relative vimentin mRNA levels were measured by quantitative PCR from within E11.5 carcass cDNA after a serial dilution of 1:1, 1:2, 1:5 and 1:10. Both linear regression analyses of semilogarithmic graphs and the direct comparison of the amount of amplified material during linear amplification accurately predicted the actual dilution levels (Table 2 and data not shown).

Hoxa-1 specific primers identified 509bp and 711bp cDNA fragments from both the distalbud and interbud regions. Identity was confirmed by Southern blot hybridization with a *Hoxa-1* specific cDNA probe (Fig. 6a). The 1.2 kb *Hoxa-1* genomic band recognized by these primers was not detected within either sample after Southern analysis. The 550bp vimentin band was used for comparative quantitation and amplified quantities, or Photosensitive Light Units (PSLs), from each designated time point were plotted on semilogarithmic graphs (Fig. 6b). Comparison of values in the linear portion of the curves demonstrated an average ratio of 1.6:1 for expression of the 711bp species between the distalbud and interbud regions (Table 3). The average ratio was calculated from four separate quantitative PCR reactions of three different

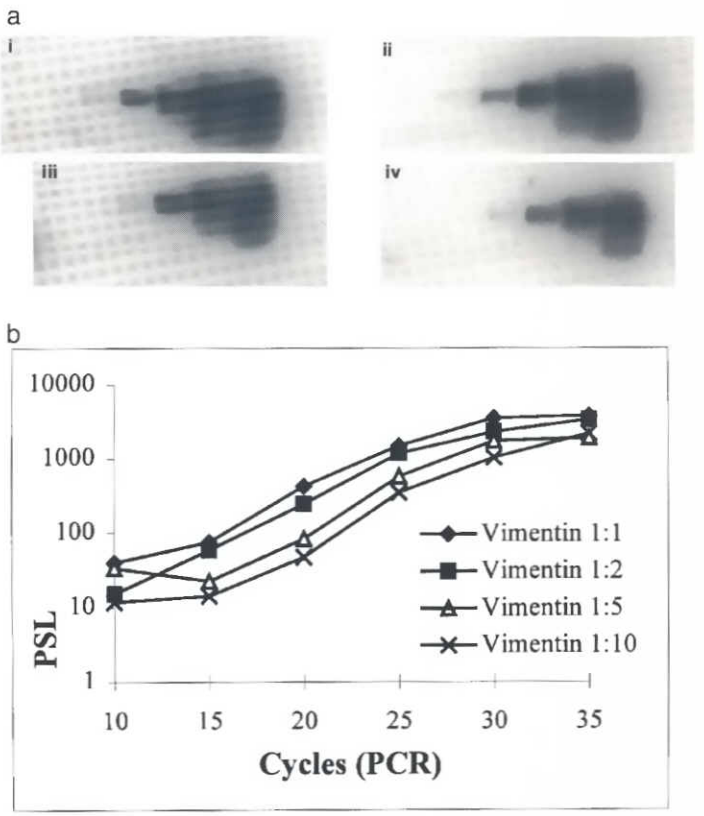

Fig. 5. Quantitation of vimentin cDNA serial dilutions by quantitative PCR. (a) *Representative phospho-image of the 550bp vimentin PCR product after Southern blot analyses. Numbers 10-35 indicate the number of PCR cycles. (i) is the 1:1 dilution; (ii) is the 1:2 dilution; (iii) is the 1:5 dilution; (iv) is the 1:10 dilution. PSL values of each amplified product from each dilution are shown in the accompanying table.* **(b)** *Semilogarithmic representation of the PSL values in each dilution series versus number of PCR cycles.*

TABLE 2

RELATIVE AMOUNTS OF VIMENTIN TRANSCRIPTS IN THE SERIAL DILUTION SAMPLES AS DETERMINED BY QUANTITATIVE PCR

a)

cDNA dilution	1:1	1:2.0	1:5.0	1:10.0
Experiment 1	1:1	1:1.4	1:5.8	1:8.5
Experiment 2	1:1	1:3.0	1:6.2	1:9.7
Experiment 3	1:1	1:2.3	1:2.3	1:6.0
Average	1:1	1:2.2	1:4.8	1:8.1

b)

cDNA dilution	1:1	1:2.0	1:5.0	1:10.0
Experiment 1	1:1	1:1.7	1:5.1	1:9.0
Experiment 2	1:1	1:1.9	1:5.4	1:7.3
Experiment 3	1:1	1:2.3	1:2.3	1:5.4
Average	1:1	1:2.0	1:4.3	1:7.2

a) Solving for No. after fitting for the linear portion of the graph (No.=the amount of starting material. See Materials and Methods. b) Ratio of PSL quantities in the linear portion of the graph.

reverse transcription procedures and demonstrated a significant difference in expression levels between the two regions (Student's *t* test, $P<0.001$). Quantitative analysis demonstrated an average ratio of 2.1:1 for expression of the 509bp species between the distalbud and interbud regions (Table 3; Student's *t* test; $P<0.001$). The average value was calculated from three separate quantitative PCR reactions of two different reverse transcription procedures. Comparison of the amount of the 711bp and 509bp transcripts demonstrated equimolar expression in the distalbud regions. They were also expressed at comparatively equimolar levels in the interbud regions (Table 4).

PCR with *Hoxa-7*, *Hoxb-6* and *Hoxb-7* specific primers identified the expected and single 589bp, 628bp and 427bp cDNA fragments, respectively, from within both the distalbud and interbud regions. Identity was confirmed by hybridization to specific cDNA probes (Figs. 7, 8, and 9). Neither the 1.59 kb *Hoxa-7* nor the 2.6 kb *Hoxb-7* genomic sequence recognized by the respective primers were amplified. Because *Hoxb-6* primers do not span an intron, the absence of genomic contamination was verified by amplification of respective interbud and distalbud reverse transcribed RNAs

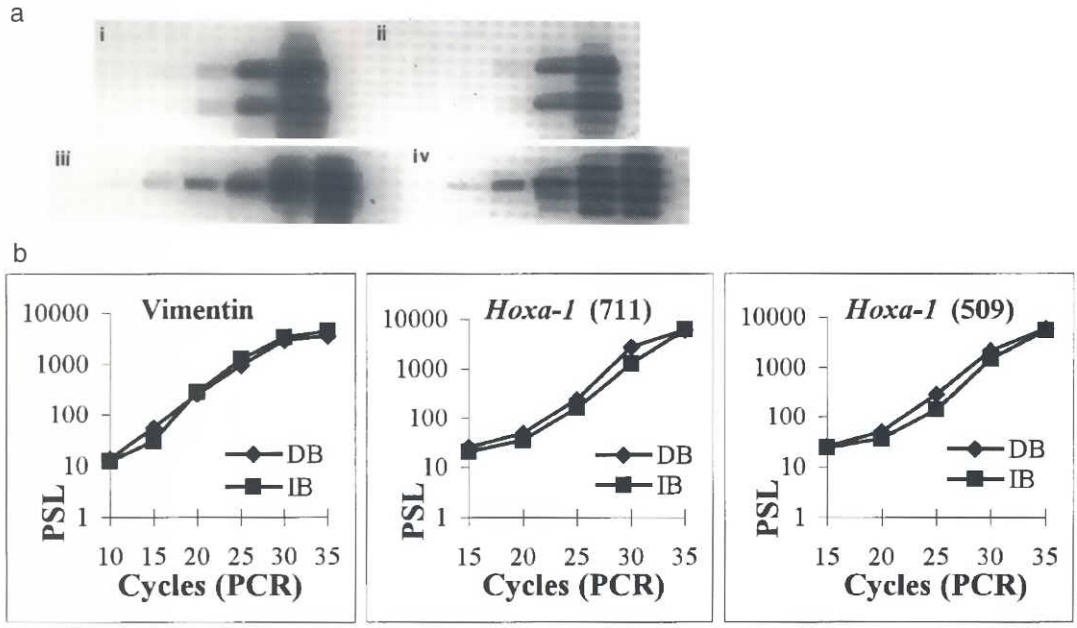

Fig. 6. Quantitation of *Hoxa-1* transcripts in distalbud versus interbud regions. *(DB) distalbud, (IB) interbud.* **(a)** *Representative phospho-image of the 711bp and 509bp Hoxa-1 and 549bp vimentin PCR products after Southern blot analysis. Numbers 10-35 indicate the number of PCR cycles. (i) DB/Hoxa-1; (ii) IB/Hoxa-1; (iii) DB/vimentin (the minor bands seen at the 30 and 35 cycle intervals respectively correspond to the size predicted for the vimentin PCR oligonucleotides); (iv) IB/vimentin.* **(b)** *PSL values of each amplified product in each region are shown on semilogarithmic graphs.*

with the *Hoxa-1* PCR primers. In all cases, the 1.2 kb *Hoxa-1* genomic fragment was not amplified (data not shown). An average ratio of 6.7:1 for *Hoxa-7* expression between the distalbud and interbud regions was calculated from three different quantitative PCR reactions of three different reverse transcription procedures (Table 3; Student's *t* test; $P<0.05$). An average ratio of 2.0:1 for *Hoxb-6* expression between the distalbud and interbud regions was calculated from five separate quantitative PCR reactions of three different reverse transcription procedures (Table 3; Student's *t* test; $P<0.01$). An average ratio of 6.0:1 for *Hoxb-7* expression between the distalbud and interbud regions was calculated from five separate quantitative PCR reactions of four different reverse transcription procedures (Table 3; Student's *t* test; $P<0.005$). Four different sets of *Hoxa-4* primers were designed, however, none were able to successfully compete for template during amplification under the specified conditions. No comparative data could, therefore, be obtained for *Hoxa-4* expression within the distalbud and interbud regions of the lung by quantitative PCR.

Discussion

This study represents the first systematic approach aimed at examining the expression of *Hox* genes specifically involved in branching morphogenesis of the embryonic mouse lung. By the use of quantitative and reverse-transcriptase PCR, Northern blot and *in situ* analyses we have demonstrated that *Hoxa-1*, *Hoxa-4*, *Hoxa-7*, *Hoxb-3*, *Hoxb-4*, *Hoxb-5*, *Hoxb-6* and *Hoxb-7* are differentially expressed both temporally and spatially during this process.

These results demonstrate that the timing of *Hoxa-1*, *Hoxa-4* and *Hoxa-7* peak expression levels is sequential during branching of the embryonic lung and correlates with their relative positions 3′ to 5′ within the *HoxA* cluster and with the different development stages of lung branching morphogenesis. *Hoxa-1* expression was only observed during the early pseudoglandular stage of development (E12.5), *Hoxa-4* peak expression correlated to the canalicular stage of development (E14.5 to E16.5) and *Hoxa-7* expression gradually increased throughout embryogenesis into the later terminal sac/alveolar stages of development. The temporal and colinear activation of *Hox* genes according to their 3' to 5' physical location within specific clusters has been noted in other systems, in particular the developing primary axis of the body, limb and intestine, where it is proposed to form an instructive protocol for the development of specific constituents (Dollé *et al.*, 1989; Izpisúa-Belmonte *et al.*, 1991a,b; Yokouchi *et al.*, 1995). Furthermore, due to the hypothesis that the relevant position of certain organs within the anteroposterior body axis represents an important factor in determining the range of homeogene transcripts they express, it has been previously suggested that a colinear scheme of *Hox* gene expression may exist in the lung (Gaunt *et al.*, 1988). Accordingly, our observations are in agreement with this latter proposal, and demonstrate that *HoxA* temporal colinearity may be a property

TABLE 3

THE RATIO OF SPECIFIC *Hox* TRANSCRIPTS IN THE DISTALBUD VERSUS INTERBUD REGIONS

	Hoxa-1(711) DB:IB	*Hoxa-1*(509) DB:IB	*Hoxa-7* DB:IB	*Hoxb-6* DB:IB	*Hoxb-7* DB: IB
Experiment 1	1.4:1	1.9:1	7.1:1	1.7:1	8.0:1
Experiment 2	1.6:1	2.0:1	3.6:1	2.9:1	4.9:1
Experiment 3	1.7:1	2.3:1	9.5:1	1.2:1	3.8:1
Experiment 4	1.5:1	*	*	1.9:1	3.6:1
Experiment 5			*	2.3:1	9.9:1
Average	1.6:1	2.1:1	6.7:1	2.0:1	6.0:1

DB, distalbud; IB, interbud. *Hoxa-1*(711): the 711bp *Hoxa-1* PCR fragment. *Hoxa-1*(509): the 509bp *Hoxa-1* PCR fragment. *Represents experiments that were discarded because «k» in the equation $y = No.e^{kx}$ did not represent a constant (see Materials and Methods). Therefore ratios could not be calculated.

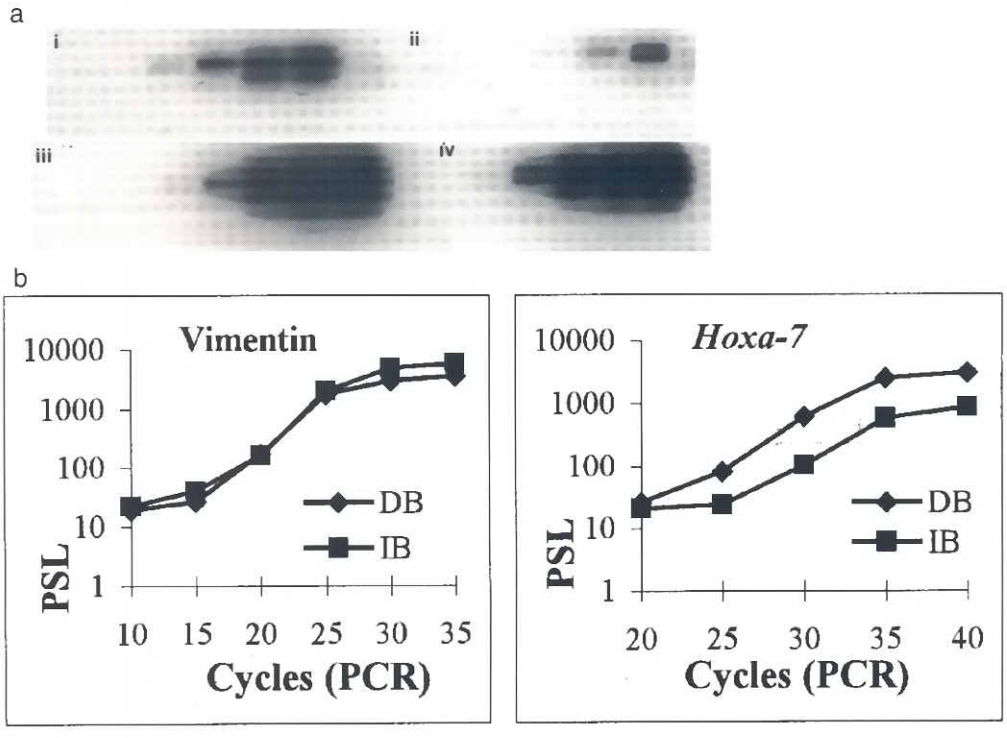

Fig. 7. Quantitation of *Hoxa-7* transcripts in distalbud versus interbud regions. *(DB) distalbud, (IB) interbud.* **(a)** *Representative phospho-image of the 589bp Hoxa-7 and 549 vimentin PCR products after Southern blot analysis. Numbers 15-40 indicate the number of PCR cycles. (i) DB/Hoxa-7; (ii) IB/Hoxa-7; (iii) DB/vimentin; (iv) IB/vimentin.* **(b)** *PSL values of each region/cDNA are shown on semilogarithmic graphs.*

regulating the stage specificity of the inductive interactions between the epithelium and the mesenchyme during lung branching morphogenesis (Taderera, 1967; Lawson, 1974; Shannon, 1994).

Temporal colinearity also appeared to be a general property of specific *HoxB* genes during development. *Hoxb-3* expression was greatest during the pseudoglandular stage of development and progressively declined. Conversely, expression of *Hoxb-4*, *Hoxb-6* and the 1.2-1.4 kb *Hoxb-7* transcript sequentially and progressively increased until greatest expression levels were observed during the terminal sac/alveolar stages of development. Greatest expression of the 1.6 kb *Hoxb-7* transcript, however, was observed at approximately E14.5, prior to that of *Hoxb-4* and *Hoxb-6*, thus representing a deviation from the general pattern of temporal colinearity observed for *Hox* genes in this and other systems. The reason for this exception is unknown, however, it is interesting that two differently sized transcripts are produced from the *Hoxb-7* gene. Whether the observed differences in *Hoxb-7* transcript sizes is attributable to alternative splicing, requires further investigation. Nevertheless, it is proposed that in the same fashion as *HoxA* gene expression domains, overlapping temporal changes in *HoxB* gene expression domains within the mesenchyme may contribute to the specification of developmental changes associated with progression through the defined maturation stages of the lung. Interestingly, previous studies have demonstrated a decrease in *Hoxb-6* expression coincident with lung development (Bogue *et al.*, 1994; Cardosa *et al.*, 1996). Whether such a discrepancy may be explained by the omission of presumptive tracheal tissue in our mRNA preparations, differences in probe specificity or the detection of alternatively spliced transcripts (we observed two differently migrating *Hoxa-1* and *Hoxb-7* transcripts by PCR Southern and Northern blot analyses, respectively), is unknown. However, we are confident that we have detected a true *Hoxb-6* transcript due to its common size with that previously described (Graham *et al.*, 1989) and, furthermore, dideoxy termination sequencing of the cDNA used as a probe verified its identity as *Hoxb-6* cDNA.

In addition to differences in temporal expression patterns, individual *Hox* genes examined by *in situ* hybridization in this study demonstrated differences in spatial mRNA localization patterns. Although such domains do not conform to the conventional rule of spatial colinearity in regard to either proximodistal or anteroposterior axes, as observed within the developing limb and axial skeleton (Izpisúa-Belmonte *et al.*, 1991b; Nohno *et al.*, 1991; Hunt and Krumlauf, 1992; Gardiner *et al.*, 1995), it is of interest that the more 5' each gene is situated within either the *HoxA* or *HoxB* cluster, the greater is its mRNA restriction in spatial localization within the E11.5 lung mesenchyme. For example, *Hoxa-1* and *Hoxb-3* mRNAs were localized at high levels throughout the mesenchyme, whereas *Hoxa-4*, *Hoxb-5* and *Hoxb-7* mRNA localization demonstrated

TABLE 4

THE RATIO OF *Hoxa-1*(711) AND *Hoxa-1*(509) TRANSCRIPTS IN THE DISTALBUD AND INTERBUD REGIONS

	DB *Hoxa-1*(711):DB *Hoxa-1* (509)	IB *Hoxa-1*(711):IB *Hoxa-1*(509)
Experiment 1	0.8:1	1.1:1
Experiment 2	1.1:1	1.3:1
Experiment 3	0.2:1	0.6:1
Average	0.7:1	1.0:1

DB, distalbud; IB, interbud. *Hoxa-1*(711): the 711bp *Hoxa-1* PCR fragment. *Hoxa-1*(509): the 509bp *Hoxa-1* PCR fragment.

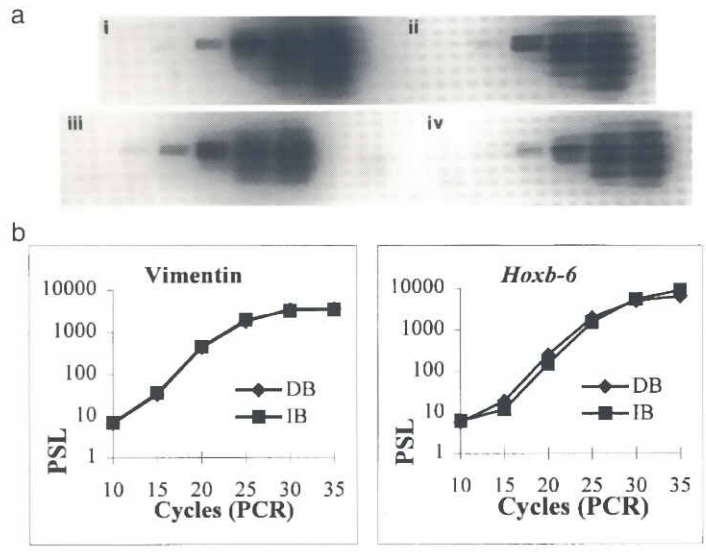

Fig. 8. Quantitation of *Hoxb-6* transcripts in distalbud versus interbud regions. *(DB) distalbud, (IB) interbud.* **(a)** *Representative phospho-image of the 628 bp Hoxb-6 and 549bp vimentin PCR products after Southern blot analysis. Numbers 10-35 indicate the number of PCR cycles. (i) DB/Hoxb-6; (ii) IB/Hoxb-6; (iii) IB/vimentin; (iv) DB/vimentin.* **(b)** *PSL values of each amplified product for each region/cDNA are shown on semilogarithmic graphs.*

comparatively greater spatial restrictions. *Hoxb-5* transcripts were observed within the periphery of the organ and immediately adjacent to the branching epithelium. Their number, however, was clearly reduced within the mesenchyme constituting the cleft regions situated between these two regions. Both *Hoxa-4* and *Hoxb-7* displayed proximodistal, or anteroposterior, gradients in mRNA localization, with greater levels being observed in the more distal reaches of the lung proper. *Hoxa-4* mRNA also demonstrated evidence of a centrifugal localization gradient; greater levels were located within the distalbud/peripheral mesenchyme than the more centrally located mesenchyme.

In accordance with these observations, quantitative PCR further demonstrated that the expression domains of more 5' *Hox* genes have greater spatial restrictions than their more 3' counterparts. *Hoxa-1* was found to be greater in the more peripheral mesenchyme, relative to the more central epithelium by *in situ* hybridization. The designed PCR primers detected two fragments which correspond to the previously described 2.2 and 2.4 kb F9 embryonal carcinoma cell *Hoxa-1* alternatively spliced transcripts (LaRosa and Gudas, 1988). Both transcripts demonstrated approximately 2 fold higher expression levels in the more peripheral distalbud regions when compared to the more central interbud regions. In contrast, *Hoxa-7* demonstrated an approximately 6.7 fold higher expression level in the distalbud regions when compared to the interbud regions after quantitative PCR. Because the detection of *Hoxa-7* PCR product from the interbud regions was only made possible after a relatively large number of PCR cycles, it is believed that expression in this domain is relatively weak. *Hoxb-6* also demonstrated an approximately 2 fold higher expression level in the distalbud regions compared to the interbud regions whereas *Hoxb-7* demonstrated approximately 6.0 fold higher expression levels in the distalbud regions when compared to the interbud regions. *In situ* analysis indicates that this difference is attributable to a relative increase within the most distal/posterior aspect of the branching lung whereas expression in the proximal/anterior aspect is very weak.

In respect to *Hoxa-1*, it is interesting that both the 509bp and 711bp fragments were detected at similar levels in the distalbud regions, and then again in the interbud regions. It is known that the NH_2-terminal 114 amino acids of the respectively translated proteins are identical, however, alternative splicing produces a truncation in one of the proteins (LaRosa and Gudas, 1988). The truncated protein does not contain the homeobox and presumably does not bind DNA. This raises the possibility that Hoxa-1 interactions during lung development may extend further than exclusively at the DNA interface.

Another interesting aspect of *Hox* mRNA spatial localization is the relative absence of *Hoxa-4* within small groups of mesenchymal cells of the distal lung regions. Although their identity was not determined, their appearance may correspond to the development of blood vessels. This suggestion is supported by the findings that a major site of *Hoxa-2* expression is in the heart outflow tracts (Patel *et al.*, 1992) and *Hoxa-3* null mutation results in carotid artery defects (Chisaka and Capechi, 1991). Such observations led to the hypothesis that these genes comprise a region of the *Hox* complex important for vasculogenesis (Patel *et al.*, 1992). Whether *Hoxa-4* plays a similar role in the developing lung remains to be determined, however, it is of interest that *Hoxa-*

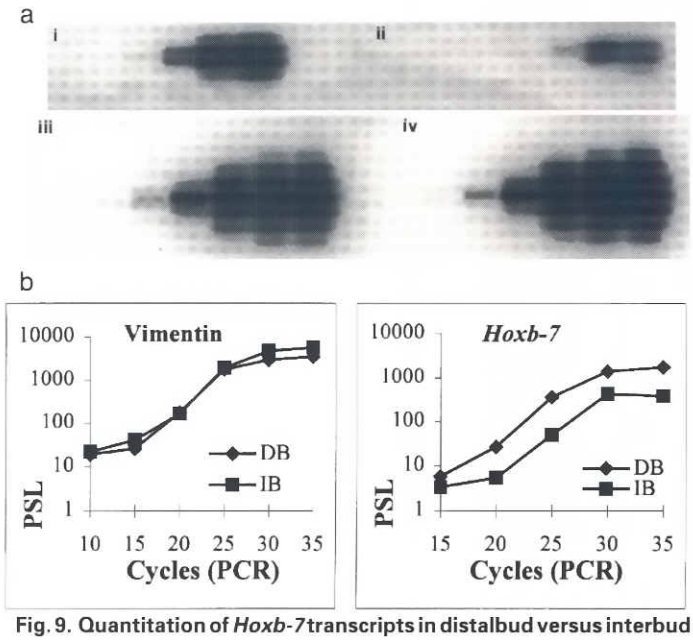

Fig. 9. Quantitation of *Hoxb-7* transcripts in distalbud versus interbud regions. *(DB) distalbud, (IB) interbud.* **(a)** *Representative phospho-image of the 427bp Hoxb-7 and 549bp vimentin PCR products after Southern blot analysis. Numbers 10-35 indicate the number of PCR cycles. (i) DB/Hoxb-7; (ii) IB/Hoxb-7; (iii) DB/vimentin; (iv) DB/vimentin.* **(b)** *PSL values of each amplified product for each region/cDNA are shown on semilogarithmic graphs.*

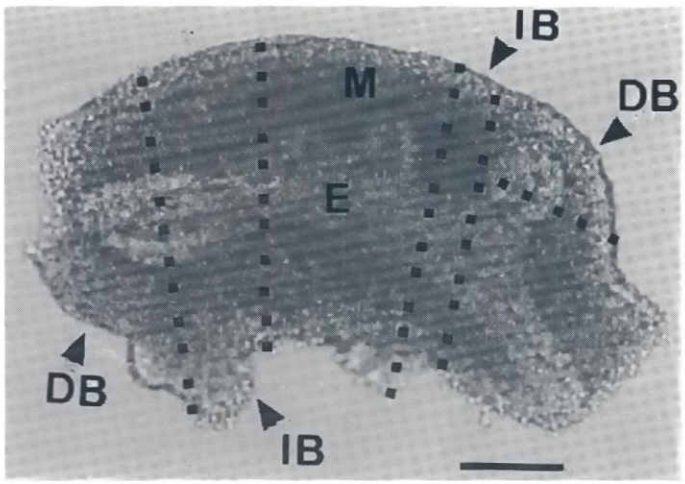

Fig. 10. Definition of interbud and distalbud regions. *E11.5 day left lung bud. Interbud (IB), distalbud (DB), epithelium (E), mesenchyme (M). Bar, 150 μm.*

2has been recently suggested to participate in lung vasculogenesis (Cardoso *et al.*, 1995).

Finally, all *Hox* genes identified by the RT-PCR technique in the E11.5 lung reside in the *HoxA* and *HoxB* clusters and are members of paralog groups 1 through to 8 only, i.e. belong to the ANT-C/*Ubx*/*abd-A* -type family of homeobox containing genes (Kessel *et al.*, 1987; Izpisúa-Belmonte *et al.*, 1991a). Interestingly, expression of *Hoxb-2*, *Hoxc-5* and *Hoxd-4* has been demonstrated previously during the earliest stages of lung morphogenesis (Gaunt *et al.*, 1989, 1990; Bogue *et al.*, 1996). *Hoxa-2* expression has been reported in the E13.5 rat lung (Cardoso *et al.*, 1995) and *Hoxa-5* has been demonstrated at E9 in the mouse, in the region of lung formation (Dony and Gruss, 1987). The expression of *Hox* genes belonging to the *Abdominal-B* family (paralogs 9-13) is still to be reported in the embryonic lung. However, *Hoxb-9* and *Hoxd-9* expression has been demonstrated by RT-PCR within the newborn lung (Bogue *et al.*, 1994). In conclusion, therefore, our findings demonstrate a temporal and colinear expression of the ANT-C/*Ubx*/*abd-A*-type *Hox* genes examined which correlates with the different stages of lung branching morphogenesis. Furthermore, although it may be too presumptuous at this stage to suggest a correspondence between the spatial distribution of transcripts and the position of respective genes in their clusters, those genes examined in this study appeared to demonstrate overlapping and progressively greater restrictions in their spatial expression domains within the mesenchyme, in accordance with their relative 5' positions within each respective cluster. In combination with previous observations it is thus conceivable that all *Hox* genes of paralogs 1 to 8 form a *Hox* code conferring position-specific regulation of the mesenchymal subsets involved in branching of the lung during organogenesis.

Materials and Methods

Mice and lung tissue

F_1(CBA/Cah x C57BL/6J) mice were mated to produce the F_2 fetuses and newborn mice obtained for all experiments. Timed pregnancies were established with the day of copulation plug designated as E0.5.

RNA purification, cDNA synthesis, PCR and subcloning

Total RNA was prepared from the branching regions of approximately 250 E11.5 lungs by guanidine hydrochloride extraction. Presumptive tracheal tissue was discarded prior to purification. Dissection was performed at the earliest gestational age possible to minimize the chances of identifying *Hox* genes exclusively associated with alveolar and bronchiolar differentiation. Integrity of the 18S and 28S ribosomal RNA was determined by denaturing gel electrophoresis of 5 μg samples (Chirgwin *et al.*, 1979; Thomas and Dziadek, 1994). mRNA was isolated using an oligo (dT) mediated magnetic capture system (PolyAtract system, Promega). Oligo (dT) primed cDNA synthesis was performed on approximately 2 μg of mRNA using a cDNA synthesis system (Promega). Before addition of the reverse-transcriptase enzyme, a negative control was made by aliquoting 10% of the mixture volume into a separate tube. *Hox* sequences were identified by PCR and Taq Track sequencing (Promega) essentially as previously described (for specific degenerate nucleotide sequences and PCR conditions, see James and Kazenwadel, 1991). A PCR negative control was created by the replacement of template with H_2O and amplified under the same conditions together with the reverse-transcriptase negative control.

cDNAs

*Eco*R1 cDNA fragments of *Hoxa-4* (0.75 kb; Galliot *et al.*, 1989), *Hoxb-3* (1.10 kb; Sham *et al.*, 1992) *Hoxb-4* (1.12 kb; Graham *et al.*, 1988) and *Hoxb-5* (1.15 kb; Krumlauf *et al.*, 1987) were subcloned into pBluescript vectors. The *Hpa*II *Hoxa-1* (0.64 kb; LaRosa and Gudas, 1988) and *Eco*RI/*Bam*HI *Hoxb-7* (0.74 kb; Meijlink *et al.*, 1987) cDNA fragments were also subcloned into pBluescript. PCR generated *Hoxa-7* (nucleotides 57-646; Kessel *et al.*, 1987), *Hoxb-6* (nucleotides 1020-1648; Schughart *et al.*, 1988) and vimentin (nucleotides 969-1518; Capetanaki *et al.*, 1990) cDNAs were subcloned into the pGEM-T vector (Promega). The identity of each cDNAs was confirmed by forward and reverse dideoxy termination sequencing.

PCR primers

Primer sites of *Hoxa-1*, *Hoxa-7* and *Hoxb-7* were designed to span intronic sequences in order to control for genomic contamination and the amplification of specific transcripts during quantitative analyses. 40 ng of each primer set was used per 1 μl of PCR reaction mixture.

i) *Hoxa-1*:
a) 5'-GAGTTGTGGTCCAAGCTATG-3' (nucleotides 347-366).
b) 5'-AGTGTCTGAGGTAGACGATG-3' (nucleotides 1039-1058).

ii) *Hoxa-7*:
a) 5'-ACCGACACTGAAAGCTGCCG-3' (nucleotides 57-76).
b) 5'-CATGCGCCGATTCTGGAACC-3' (nucleotides 627-646).

iii) *Hoxb-6*:
a) 5'-TAATCGCTACCTGACCCGCC-3' (nucleotides 1020-1039).
b) 5'-GCTCCTTCCAGTGGCTTTGG-3' (nucleotides 1629-1648).

iv) *Hoxb-7*:
a) 5'-GTTCCTTCAACATGCACTGC-3' (nucleotides 571-590).
b) 5'-TTCCTCCTCTTGGCTTTCTC-3' (nucleotides 979-998).

v) Vimentin:
a) 5'-CAAGTTTGCTGACCTCTCTG-3' (nucleotides 969-988).
b) 5'-ACTGTTGCACCAAGTGTGTG-3' (nucleotides 1499-1518).

Northern blot analysis

Total RNA and mRNA were isolated from the branching regions of E12.5, E13.5, E14.5, E15.5, E16.5, E17.5, E18.5 and newborn mouse lungs, according to methods described above. A 28S oligonucleotide

(GACTCGCGCACGCGTTAGACTCCTTGGTCC) and the cDNAs were end-labeled and randomly primed with [α-^{32}P]dCTP, respectively. Northern gel analyses were performed according to standard methods (Sambrook *et al.*, 1989). For *Hox* quantitation, one filter was probed sequentially with two different *Hox* cDNAs and the vimentin cDNA. Temporal differences in the expression levels of each *Hox* gene were analyzed by either linear or quadratic regression analysis where applicable. The *P* value that tests the null hypothesis of whether the linear slope between the selected points would be as far from zero if the points were randomly selected is reported. The *P* value was calculated from an F test. The temporal expression pattern of each *Hox* gene was analyzed twice, except for *Hoxa-4* which was analyzed once.

In situ hybridization analysis

In situ hybridization was performed as previously described (Thomas and Dziadek, 1994). cRNA probes were generated by transcription of linearized DNA with either SP6, T6 or T7 polymerase incorporating [α-^{33}P]dCTP. Hybridized and dehydrated sections were exposed to Kodak K-OMAT for 2 days. Those showing low background were coated with 50% emulsion (Ilford) in 2% glycerol for 10-14 days. At least 17 different sections from 6 different lungs were hybridized with each antisense riboprobe. Every sixth section was hybridized with the corresponding sense probe. In the case of *Hoxb-3* the specificity of antisense riboprobe hybridization was determined by comparing the hybridization of *Hoxb-5* sense riboprobe. Hybridization with sense riboprobe gave levels only slightly higher than the background fogging of the emulsion. In each case, distinctions could be made between the pattern of hybridization produced by each of the 5 antisense riboprobes and that of their corresponding sense riboprobes. It is, therefore, concluded that specific spatial expression patterns for each gene were detected by this technique.

Quantitative PCR analysis

Quantitative PCR was performed according to a modification of previously described methods (Kay *et al.*, 1993; Yokoi *et al.*, 1993; Zachar *et al.*, 1993). At least 100 E11.5 mouse lungs were dissected with tungsten needles into distal budding (distalbud) and cleft (interbud) regions (Fig. 10). Individual cDNA mixtures were prepared from 1.5 μg of total distalbud, interbud and carcass RNA, each in a final volume of 20 μl.

Vimentin Control Experiment:

Ten μl of carcass cDNA was serially diluted 1:1, 1:2, 1:5 and 1:10 to determine the suitability of quantitative PCR for this system. Briefly, 550 μl PCR mixture (Bresatec) minus template was prepared batched, 20 μl was removed for a negative control and the remainder was divided into 4 equal 130 μl portions. 10 μl of each serial dilution was added to individual 130 μl portions. Each portion was subdivided into separate 20 μl aliquots and then subjected to PCR at an annealing temperature of 58°C. Four 20 μl aliquots, representing each of the serially diluted cDNAs, were removed every 5 cycles for 35 cycles. Amplified DNA was resolved by agarose gel electrophoresis, alkaline transferred to Hybond C-nylon membranes (Amersham) and probed in RapidHyb (Amersham) with randomly primed [α-^{32}P]dCTP-labeled vimentin cDNA according to standard methods (Sambrook *et al.*, 1989). Relative values of amplified material were obtained by phosphorimage analysis and plotted on semilogarithmic graphs as PCR product (Photosensitive Light Units or PSLs)/PCR reaction cycle number. DNA was never amplified from negative controls. Relative values of starting material were calculated by linear regression analysis according to the equation $y = No.e^{kx}$, where «y» represents yield, «No.» represents the amount of starting material, «k» represents the efficiency of amplification and «x» represents the number of cycles (Yokoi *et al.*, 1993; Zachar *et al.*, 1993 and data not shown). Values were also calculated by comparing the PSL values directly from within the linear portion of the graph.

Hox quantitation

Six μl of distalbud and interbud cDNAs were added to separate portions of identically prepared PCR mixture, containing both vimentin and *Hox* specific primers. Each portion was then divided into 20 μl aliquots and subjected to PCR at an annealing temperature of 58°C. One distalbud and 1 interbud PCR reaction tube was removed every 5 cycles until the PCR reaction reached a plateau. 1x5 μl and 1x12 μl samples from each tube were subjected to gel electrophoresis, DNA was transferred to nylon membranes and then probed for vimentin or the *Hox* gene in question, respectively. PSL values were plotted on semilogarithmic graphs and the relative starting amount of each *Hox* gene was determined by comparing the PSL values from within the linear portion of each curve. Trial vimentin PCR reactions of both the distalbud and interbud prepared cDNAs were performed to ensure that between samples, the vimentin internal control was amplified at a similar rate (data not shown). The calculation of *Hox* ratios between samples was only performed when PSL quantities could be assessed at the same cycle number and the corresponding vimentin standards displayed similar kinetics throughout the amplification procedure. Pipetting errors, differences in reverse transcription preferences and PCR sample inhibitor concentrations, and differences in the efficiencies of electrophoresis, blotting, hybridization, and phospho-imaging analysis were controlled for by repetitive experimentation utilizing different RNA preparations and reverse transcription procedures. All amplified material from each experiment was electrophoresed on the same gel and, therefore, blotted under the same conditions. All hybridizations were performed with an excess of [α-^{32}P]dCTP-labeled specific randomly-primed cDNA probes. Hybridization was performed in the same buffer at the same time for filters to be probed for the same cDNA. In each case primers did not amplify DNA from either the PCR negative control nor from the reverse transcription negative control.

Quantitation of hybridized probes

Northern and PCR-Southern blot quantitation was performed by phospho-imaging analysis on a Bio imaging analyzer (Fuji BAS 1000). Measurements were made in PSLs. Exposure times were between 5 and 15 min for PCR reactions and 1 and 3 days for Northern blots.

Acknowledgments

We are grateful to Prof. David de Kretser and Prof. Manuel Mark for generous advice and critical reading of the manuscript. We also thank Rob James for the kind donation of PCR oligonucleotides, Chris Wright and Nancy Manley for the kind donation of Hoxa-1, Hoxb-3, Hoxb-4, Hoxb-5, and Hoxb-6 and Hoxa-3 cDNAs, respectively, Aden Sudsbury and Norbert Ghyselinck for statistical advice and Bernard Boulay for assistance with photography. This work was supported by funding from the Australian Research Council.

References

BARON, A., FEATHERSTONE, M.S., HILL, R.E., HALL, A., GALLIOT, B. and DUBOULE, D. (1987). Hox-1.6: a mouse homeo-box-containing gene member of the Hox-1 complex. *EMBO J. 6:* 2977-2986.

BEHRINGER, R.R., CROTTY, D.A., TENNYSON, V.M., BRINSTER, R.L., PALMITER, R.D. and WOLGEMUTH, D.J. (1993). Sequences 5' of the homeobox of the Hox-1.4 gene direct tissue-specific expression of lacZ during mouse development. *Development 117:* 823-833.

BELLUSCI, S., HENDERSON, R., WINNIER, G., OIKAWA, T. and HOGAN, B.L. (1996). Evidence for normal expression and targeted misexpression that bone morphogenetic protein (Bmp-4) plays a role in mouse embryonic lung morphogenesis. *Development 122:* 1693-1702.

BERNACKI, S.H., NERVI, C., VOLLBERG, T.M. and JETTEN, A.M. (1992). Homeobox 1.3 expression: induction by retinoic acid in human bronchial fibroblasts. *Am. J. Respir. Cell Mol. Biol. 7:* 3-9.

BERNFIELD, M. (1981). Organisation and remodelling of the extracellular matrix in morphogenesis. In *Morphogenesis and Pattern Formation: Implications for Normal and Abnormal Development* (Eds. L. Brinkley, B.M. Carlson and G. Connelly). Raven Press, New York, pp. 139-162.

BOGUE, C.W., GROSS, I., VASAVADA, H., DYNIA, D.W., WILSON, C.M. and JACOBS, H.C. (1994). Identification of Hox genes in newborn lung and effects of

gestational age and retinoic acid on their expression. *Am. J. Physiol. 266:* L448-L454.

BOGUE, C.W., LOU L.J., VASAVADA, H., WILSON, C.M. and JACOBS, H.C. (1996). Expression of Hoxb genes in the developing mouse foregut and lung. *Am. J. Respir. Cell. Mol. Biol. 15:* 163-171.

CAPETANAKI, Y., KUISK, I., ROTHBLUM, K. and STARNES, S. (1990). Mouse vimentin: structural relationship to c-fos, jun, CREB and tpr. *Oncogene 5:* 645-655.

CAPOVILLA, M., BRANDT, M. and BOTAS, J. (1994). Direct regulation of decapentaplegic by Ultrabithorax and its role in *Drosophila* midgut morphogenesis. *Cell 76:* 461-475.

CARDOSO, W.V. (1995). Transcription factors and pattern formation in the developing lung. *Am. J. Physiol. 269:* L429-L442.

CARDOSO, W.V., MITSIALIS, S.A., BRODY, F.S. and WILLIAMS, M.C. (1996). Retinoic acid alters the expression of pattern-related genes in the developing rat lung. *Dev. Dynamics 207:* 47-59.

CHIRGWIN, J.M., PRZYBYLA, A.E., MACDONALD, R.J. and RUTTER, N.J. (1979). Isolation of biologically active ribonucleic acid from sources enriched with ribonuclease. *Biochemistry 18:* 5294-5299.

CHISAKA, O. and CAPECCHI, M.R. (1991). Regionally restricted developmental defects resulting from targeted disruption of the mouse homeobox gene hox-1.5. *Nature 350:* 473-479.

DOLLÉ, P., IZPISUA-BELMONTE, J.C., BROWN, J., TICKLE, C. and DUBOULE, D. (1993). Hox genes and the morphogenesis of the vertebrate limb. *Prog. Clin. Biol. Res. 383A:* 11-20.

DOLLÉ, P., IZPISUA-BELMONTE, J.C., FALKENSTEIN, H., RENUCCI, A. and DUBOULE, D. (1989). Coordinate expression of the murine Hox-5 complex homeobox-containing genes during limb pattern formation. *Nature 342:* 767-772.

DONY, C. and GRUSS, P. (1987). Specific expression of the Hox 1.3 homeo box gene in murine embryonic structures originating from or induced by the mesoderm. *EMBO J. 6:* 2965-2975.

DUBOULE, D. (1995). Vertebrate Hox genes and proliferation: an alternative pathway to homeosis? *Curr. Opin. Genet. Dev. 5:* 525-528.

EKBLOM, P., EKBLOM, M., FECKER, L., KLEIN, G., ZHANG, H.Y., KADOYA, Y., CHU, M.L., MAYER, U. and TIMPL, R. (1994). Role of mesenchymal nidogen for epithelial morphogenesis *in vitro*. *Development 120:* 2003-2014.

FRIEDMANN, Y., DANIEL, C.A., STRICKLAND, P. and DANIEL, C.W. (1994). Hox genes in normal and neoplastic mouse mammary gland. *Cancer Res. 54:* 5981-5985.

GALLIOT, B., DOLLÉ, P., VIGNERON, M., FEATHERSTONE, M.S., BARON, A. and DUBOULE, D. (1989). The mouse Hox-1.4 gene: primary structure, evidence for promoter activity and expression during development. *Development 107:* 343-359.

GARDINER, D.M., BLUMBERG, B., KOMINE, Y. and BRYANT, S.V. (1995). Regulation of HoxA expression in developing and regenerating axolotl limbs. *Development 121:* 1731-1741.

GAUNT, S.J., COLETTA, P.L., PRAVTCHEVA, D. and SHARPE, P.T. (1990). Mouse Hox-3.4: homeobox sequence and embryonic expression patterns compared with other members of the Hox gene network. *Development 109:* 329-339.

GAUNT, S.J., KRUMLAUF, R. and DUBOULE, D. (1989). Mouse homeo-genes within a subfamily, Hox-1.4, -2.6 and -5.1, display similar anteroposterior domains of expression in the embryo, but show stage- and tissue-dependent differences in their regulation. *Development 107:* 131-141.

GAUNT, S.J., SHARPE, P.T. and DUBOULE, D. (1988). Spatially restricted domains of homeo-gene transcripts in mouse embryos: relation to a segmented body plan. *Development 104 (Suppl.):* 169-179.

GRAHAM, A., PAPALOPULU, N. and KRUMLAUF, R. (1989). The murine and *Drosophila* homeobox gene complexes have common features of organization and expression. *Cell 57:* 367-378.

GRAHAM, A., PAPALOPULU, N., LORIMER, J., MCVEY, J.H., TUDDENHAM, E.G. and KRUMLAUF, R. (1988). Characterization of a murine homeo box gene, Hox-2.6, related to the *Drosophila* Deformed gene. *Genes Dev. 2:* 1424-1438.

HE, X., TREACY, M.N., SIMMONS, D.M., INGRAHAM, H.A., SWANSON, L.W. and ROSENFELD, M.G. (1989). Expression of a large family of POU-domain regulatory genes in mammalian brain development [published erratum in *Nature* 1989, Aug 24, *340*(6235):662]. *Nature 340:* 35-41.

HILFER, S.R., RAYNER, R.M. and BROWN, J.W. (1985). Mesenchymal control of branching pattern in the fetal mouse lung. *Tissue Cell 17:* 523-538.

HUNT, P. and KRUMLAUF, R. (1992). Hox codes and positional specification in vertebrate embryonic axes. *Annu. Rev. Cell Biol. 8:* 227-256.

IZPISÚA-BELMONTE, J.C., BROWN, J.M., DUBOULE, D. and TICKLE, C. (1992). Expression of Hox-4 genes in the chick wing links pattern formation to the epithelial-mesenchymal interactions that mediate growth. *EMBO J. 11:* 1451-1457.

IZPISÚA-BELMONTE, J.C., FALKENSTEIN, H., DOLLÉ, P., RENUCCI, A. and DUBOULE, D. (1991a). Murine genes related to the *Drosophila* AbdB homeotic genes are sequentially expressed during development of the posterior part of the body. *EMBO J. 10:* 2279-2289.

IZPISÚA-BELMONTE, J.C., TICKLE, C., DOLLÉ, P., WOLPERT, L. and DUBOULE, D. (1991b). Expression of the homeobox Hox-4 genes and the specification of position in chick wing development. *Nature 350:* 585-589.

JAMES, R. and KAZENWADEL, J. (1991). Homeobox gene expression in the intestinal epithelium of adult mice. *J. Biol. Chem. 266:* 3246-3251.

JONES, F.S., PREDIGER, E.A., BITTNER, D.A., DE ROBERTIS, E.M. and EDELMAN, G.M. (1992). Cell adhesion molecules as targets for Hox genes: neural cell adhesion molecule promoter activity is modulated by cotransfection with Hox-2.5 and -2.4. *Proc. Natl. Acad. Sci. USA 89:* 2086-2090.

KADOYA, Y., KADOYA, K., DURBEEJ, M., HOLMVALL, K., SOROKIN, L. and EKBLOM, P. (1995). Antibodies against domain E3 of laminin-1 and integrin alpha 6 subunit perturb branching epithelial morphogenesis of submandibular gland, but by different modes. *J. Cell Biol. 129:* 521-534.

KAY, G.F., PENNY, G.D., PATEL, D., ASHWORTH, A., BROCKDORFF, N. and RASTAN, S. (1993). Expression of Xist during mouse development suggests a role in the initiation of X chromosome inactivation. *Cell 72:* 171-182.

KESSEL, M., SCHULZE, F., FIBI, M. and GRUSS, P. (1987). Primary structure and nuclear localization of a murine homeodomain protein. *Proc. Natl. Acad. Sci. USA 84:* 5306-5310.

KONGSUWAN, K., WEBB, E., HOUSIAUX, P. and ADAMS, J.M. (1988). Expression of multiple homeobox genes within diverse mammalian haemopoietic lineages. *EMBO J. 7:* 2131-2138.

KRUMLAUF, R., HOLLAND, P.W., MCVEY, J.H. and HOGAN, B.L. (1987). Developmental and spatial patterns of expression of the mouse homeobox gene, Hox 2.1. *Development 99:* 603-617.

LAROSA, G.J. and GUDAS, L.J. (1988). Early retinoic acid-induced F9 teratocarcinoma stem cell gene ERA-1: alternate splicing creates transcripts for a homeobox-containing protein and one lacking the homeobox. *Mol. Cell. Biol. 8:* 3906-3917.

LAWSON, K.A. (1974). Mesenchyme specificity in rodent salivary gland development: the response of salivary epithelium to lung mesenchyme *in vitro*. *J. Embryol. Exp. Morphol. 32:* 469-493.

LAWSON, K.A. (1983). Stage specificity in the mesenchyme requirement of rodent lung epithelium *in vitro*: a matter of growth control? *J. Embryol. Exp. Morphol. 74:* 183-206.

LONAI, P., ARMAN, E., CZOSNEK, H., RUDDLE, F.H. and BLATT, C.(1987). New murine homeoboxes: structure, chromosomal alignment, and differential expression in adult erythropoiesis. *DNA 6:* 409-418.

MEIJLINK, F., DE LAAF, R., VERRIJZER, P., DESTREE, O., KROEZEN, V., HILKENS, J. and DESCHAMPS, J. (1987). A mouse homeobox containing gene on chromosome 11: sequence and tissue-specific expression. *Nucleic Acids. Res. 15:* 6773-6786.

MENDELSOHN, C., LOHNES, D., DECIMO, D., LUFKIN, T., LEMEUR, M., CHAMBON, P. and MARK, M. (1994). Function of the retinoic acid receptors (RARs) during development (II). Multiple abnormalities at various stages of organogenesis in RAR double mutants. *Development 120:* 2749-2771.

NOGAWA, H. and ITO, T. (1995). Branching morphogenesis of embryonic mouse lung epithelium in mesenchyme-free culture. *Development 121:* 1015-1022.

NOHNO, T., NOJI, S., KOYAMA, E., OHYAMA, K., MYOKAI, F., KUROIWA, A., SAITO, T. and TANIGUCHI, S. (1991). Involvement of the Chox-4 chicken homeobox genes in determination of anteroposterior axial polarity during limb development. *Cell 64:* 1197-1205.

ODENWALD, W.F., TAYLOR, C.F., PALMER-HILL, F.J., FRIEDRICH, V.Jr., TANI, M. and LAZZARINI, R.A. (1987). Expression of a homeo domain protein in non-contact inhibited cells and postmitotic neurons. *Genes Dev. 1:* 482-496.

PANZER, S., WEIGEL, D. and BECKENDORF, S.K. (1992). Organogenesis in *Drosophila melanogaster*: embryonic salivary gland determination is controlled by homeotic and dorsoventral patterning genes. *Development 114:* 49-57.

PARIKH, H., SHAH, S., HILT, D. and PETERKOFSKY, A. (1995). Organization, sequence and regulation of expression of the murine Hoxa-7 gene. *Gene 154:* 237-242.

PATEL, C.V., GORSKI, D.H., LEPAGE, D.F., LINCECUM, J. and WALSH, K. (1992). Molecular cloning of a homeobox transcription factor from adult aortic smooth muscle. *J. Biol. Chem. 267:* 26085-26090.

PETERS, K., WERNER, S., LIAO, X., WERT, S., WHITSETT, J. and WILLIAMS, L. (1994). Targeted expression of a dominant negative FGF receptor blocks branching morphogenesis and epithelial differentiation of the mouse lung. *EMBO J. 13:* 3296-3301.

ROMAN, J., CROUCH, E.C. and McDONALD, J.A. (1991). Reagents that inhibit fibronectin matrix assembly of cultured cells also inhibit lung branching morphogenesis *in vitro*. Implications for lung development, injury and repair. *Chest 99:* 20S-21S.

ROSS, S.A., AHRENS, R.A. and DE LUCA, L.M. (1994). Retinoic acid enhances adhesiveness, laminin and integrin beta 1 synthesis, and retinoic acid receptor expression in F9 teratocarcinoma cells. *J. Cell. Physiol. 159:* 263-273

SAMBROOK, J., FRITSCH, E.F. and MANIATIS, T. (Eds.) (1989). *Molecular Cloning: A Laboratory Manual,* second ed. Cold Spring Harbor Laboratory Press, Cold Spring Harbor.

SAXÉN, L., LEHTONEN, E., KARKINEN-JAASKELAINEN, M., NORDLING, S. and WARTIOVAARA, J. (1976). Are morphogenetic tissue interactions mediated by transmissible signal substances or through cell contacts? *Nature 259:* 662-663.

SCHUGER, L., SKUBITZ, A.P., DE LAS MORENAS, A. and GILBRIDE, K. (1995). Two separate domains of laminin promote lung organogenesis by different mechanisms of action. *Dev. Biol. 169:* 520-532.

SCHUGHART, K., UTSET, M.F., AWGULEWITSCH, A. and RUDDLE, F.H. (1988). Structure and expression of Hox-2.2, a murine homeobox-containing gene. *Proc. Natl. Acad. Sci. USA 85:* 5582-5586.

SETH, R., SHUM, L., WU, F., WUENSCHELL, C., HALL, F.L., SLAVKIN, H.C. and WARBURTON, D. (1993). Role of epidermal growth factor expression in early mouse embryo lung branching morphogenesis in culture: antisense oligodeoxynucleotide inhibitory strategy. *Dev. Biol. 158:* 555-559.

SHAM, M.H., HUNT, P., NONCHEV, S., PAPALOPULU, N., GRAHAM, A., BONCINELLI, E. and KRUMLAUF, R. (1992). Analysis of the murine Hox-2.7 gene: conserved alternative transcripts with differential distributions in the nervous system and the potential for shared regulatory regions. *EMBO J. 11:* 1825-1836.

SHANNON, J.M. (1994). Induction of alveolar type II cell differentiation in fetal tracheal epithelium by grafted distal lung mesenchyme. *Dev. Biol. 166:* 600-614.

SHEN, W.F., DETMER, K., SIMONITCH-EASON, T.A., LAWRENCE, H.J. and LARGMAN, C. (1991). Alternative splicing of the Hox2.2 homeobox gene in human hematopoeitic cells and murine embryonic and adult tissues. *Nucleic Acids Res. 19:* 539-545.

SHEN, W.F., LARGMAN, C., LOWNEY, P., HACK, F.M. and LAWRENCE, H.J. (1989). Expression of homeobox genes in human erythroleukemia cells. *Adv. Exp. Med. Biol. 271:* 211-219.

SOUZA, P., KULISZEWSKI, M., WANG, J., TSEU, I., TANSWELL, A.K. and POST, M. (1995). PDGF-AA and its receptor influence early lung branching via an epithelial-mesenchymal interaction. *Development 121:* 2559-2567.

TADERERA, J.V. (1967). Control of lung differentiation *in vitro*. *Dev. Biol. 16:* 489-512.

THOMAS, T. and DZIADEK, M. (1994). Expression of collagen alpha 1(IV), laminin and nidogen genes in the embryonic mouse lung: implications for branching morphogenesis. *Mech. Dev. 45:* 193-201.

VASIOS, G.W., GOLD, J.D., PETKOVICH, M., CHAMBON, P. and GUDAS, L.J. (1989). A retinoic acid-responsive element is present in the 5' flanking region of the laminin B1 gene. *Proc. Natl. Acad. Sci. USA 86:* 9099-9103

YOKOI, H., NATSUYAMA, S., IWAI, M., NODA, Y., MORI, T., MORI, K.J., FUJITA, K., NAKAYAMA, H. and FUJITA, J. (1993). Non-radioisotopic quantitative RT-PCR to detect changes in mRNA levels during early mouse embryo development. *Biochem. Biophys. Res. Commun. 195:* 769-775.

YOKOUCHI, Y., SAKIYAMA, J. and KUROIWA, A. (1995). Coordinated expression of Abd-B subfamily genes of the HoxA cluster in the developing digestive tract of chick embryo. *Dev. Biol. 169:* 76-89.

ZACHAR, V., THOMAS, R.A. and GOUSTIN, A.S. (1993). Absolute quantitation of target DNA: a simple competitive PCR for efficient analysis of multiple samples. *Nucleic Acids Res. 21:* 2017-2018.

Received: May 1997
Accepted for publication: June 1997